

Morphology and chemical composition of γ/γ' phases in Re-containing Ni-based single crystal superalloy during two-step aging

WANG Jing, ZHANG Lan-ting, CHEN Ke, SUN Nai-rong, SHAN Ai-dang

School of Materials Science and Engineering, Shanghai Jiao Tong University, Shanghai 200240, China

Received 18 October 2010; accepted 16 December 2010

Abstract: The γ/γ' microstructure of a Re-containing Ni-based single crystal super alloy after a two-step aging was studied using scanning electron microscopy (SEM), transmission electron microscopy (TEM) and scanning transmission electron microscopy (STEM). The crystals were grown by the floating zone (FZ) method. Both cuboidal and spherical γ' precipitates were formed after a two-step aging. The size of the cuboidal γ' phases first increased and then decreased with the extension of the second-step aging time. Re, Co and Cr strongly concentrated in the γ phase whereas Ni and Al enriched in the γ' phase. Thermodynamic calculation by JMatPro was performed to explain the experimental observations.

Key words: Ni-based single-crystal superalloy; γ/γ' microstructure; elemental distribution; heat treatment; JMatPro calculation

1 Introduction

Ni-based single-crystal superalloys, which consist of a high volume fraction of ordered $L1_2$ γ' precipitates coherent with the disordered FCC γ matrix, are widely used for turbine engine blades employed for jet propulsion where superior high-temperature strength and creep resistance are required [1–4]. The morphology, size and distribution of the γ' precipitates in the γ matrix of Ni-based single-crystal superalloys have been shown to drastically influence the high-temperature creep properties [5–7]. Heat treatment is important to obtain a desired γ/γ' microstructure [8]. Therefore, it is essential to study the γ/γ' microstructure evolution during heat treatment. Moreover, a certain amount of refractory elements such as Re, W, Mo and Co for both solid-solution strengthening in the γ matrix and precipitation strengthening via the γ' formation, are added to enhance the high-temperature creep properties [9–11]. Furthermore, the precipitate morphology, lattice misfit and composition of the γ/γ' phases are interrelated [12]. Thus investigation of the elemental partitioning behavior of the γ/γ' phases could clarify the relationship between the nominal alloy composition and the local chemistry in γ/γ' phases. This may shed light on the

maximum benefits of the alloying elements. In the present investigation, the morphology and chemical composition of the γ/γ' phases in a Re-containing Ni-based single-crystal superalloy after two-step aging were studied.

2 Experimental

Polycrystalline rod ingots of a superalloy with a nominal composition (mass fraction, %) of Ni-6.0Al-12.0W-12.0Co-5.0Re-2.0Mo-3.0Cr-0.1Hf were prepared by arc-melting high pure metals (99.99%) in Ar atmosphere. Single crystals with approximate 10 mm in diameter and 30 mm in length were grown in a laboratory optical-heating floating zone apparatus (Asgal FZ-20035WHV) at a growth rate of 2.5 mm/h. Necking was performed twice so that the growth direction was close to [001]. The thermodynamic properties of the crystal were calculated using JMatPro with the latest relevant database for Ni-based superalloys. The as-grown crystals were solution treated at 1300 °C for 1 h and at 1320 °C for 5 h, followed by air cooling. Subsequently, the crystals were aged at 1100 °C for 4 h followed by air cooling (first-step aging). Finally, the crystals were aged at 870 °C for 25 h, 35 h and 40 h, respectively (second-step aging).

Back-scattered electron (BSE) images were taken in the as-polished state to observe the γ/γ' microstructure on a JEOL JSM-7600F scanning electron microscope (SEM). Specimens for transmission electron microscopy (TEM) were first mechanically ground to about 20 μm in thickness and then finally thinned by ion milling. Details of the γ/γ' microstructure were investigated on a JEOL JEM-2100F equipped with energy dispersive X-ray spectrometer (EDS). The elemental distribution in the γ/γ' phases was investigated on scanning transmission electron microscope (STEM).

3 Results

3.1 As-grown γ/γ' microstructure

The microstructures of the as-grown crystal are shown in Fig. 1. In the low-magnification BSE image

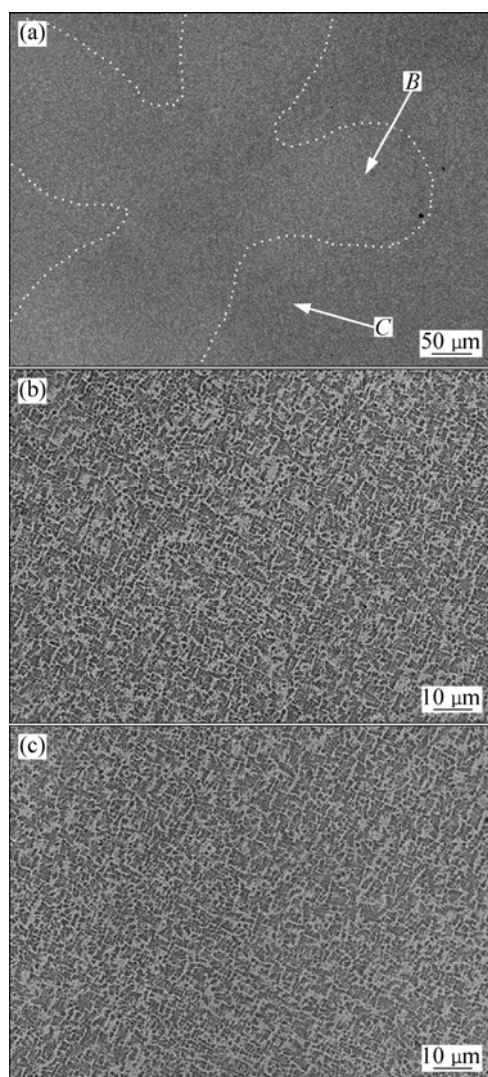


Fig. 1 BSE micrographs of as-grown crystals: (a) Low-magnification image showing weak dendrite pattern (boundary of dendrite is sketched by dotted lines); (b) γ/γ' microstructure in dendrite cores; (c) γ/γ' microstructure in interdendritic regions

(Fig. 1(a)), the light gray areas are the dendrite cores (arrow B) and the darker areas (arrow C) are the interdendritic regions. However, because of the small difference in composition, they cannot be clearly distinguished in Fig. 1(a). Details of the γ/γ' microstructure in the dendrite cores (Fig. 1(b)) and in the interdendritic regions (Fig. 1(c)) are almost the same. Moreover, no γ - γ' eutectic areas were found, indicating that there was no obvious chemical segregation in the as-grown crystals. Compared with the Bridgeman method [13], the crystals grown by the FZ method are more uniform in the microstructure.

3.2 γ/γ' microstructure after heat treatment

Figure 2 shows the γ/γ' microstructures of the crystals after aging. In the BSE images, the bright area is the γ matrix and the dark area is the γ' phase. Cuboidal γ' precipitates of 200–400 nm aligned along the $\langle 001 \rangle$ direction were found in the crystals after the first-step aging (Fig. 2(a)). The volume fraction of the γ' phase was estimated to be about 40%. The γ/γ' microstructures after second-step aging at 870 $^{\circ}\text{C}$ for 25 h, 35 h and 40 h are shown in Figs. 2(a), (b) and (c), respectively. Figure 2(b) shows two types of the γ' precipitates in the microstructure: cuboidal ones with sizes of 180–500 nm and very fine spherical ones with sizes of about 50 nm. The volume fraction of the γ' phase was estimated to be about 56%. In Fig. 2(c), the size of cuboidal γ' precipitates increased obviously to 200–600 nm. Furthermore, some needle-shaped γ phases (arrow A in Fig. 2(c)) inside the cuboidal γ' precipitates were observed. The volume fraction of the γ' phase was estimated to be about 61%. However, with the increase of aging time, the γ/γ' microstructure of the crystal became homogeneous (Fig. 2(d)). The microstructure is composed of cuboidal γ' precipitates with sizes of 250–300 nm with a spacing of about 100 nm, as shown in Fig. 2(d). Only a tiny amount of spherical γ' precipitates were observed. The volume fraction of the γ' phase was estimated to be about 69%.

3.3 Influence of aging on γ/γ' phases

Figure 3 shows dark-field STEM images of the γ/γ' microstructures and chemical composition distribution across the γ/γ' interface after the first-step aging and the second-step aging for 25 h. Similar to the BSE image, the bright area is the γ matrix and the black area is the γ' phase. Figure 3(a) shows very fine precipitates in the γ matrix after the first-step aging, which are not observed in Fig. 2(a). Composition analysis across the wide γ matrix containing fine precipitates (the white dashed line in Fig. 3(a)) indicates that these fine precipitates are rich in Re, Co, Cr and Mo, and depleted in Ni and Al (indicated by shaded regions of A, B, C shown in

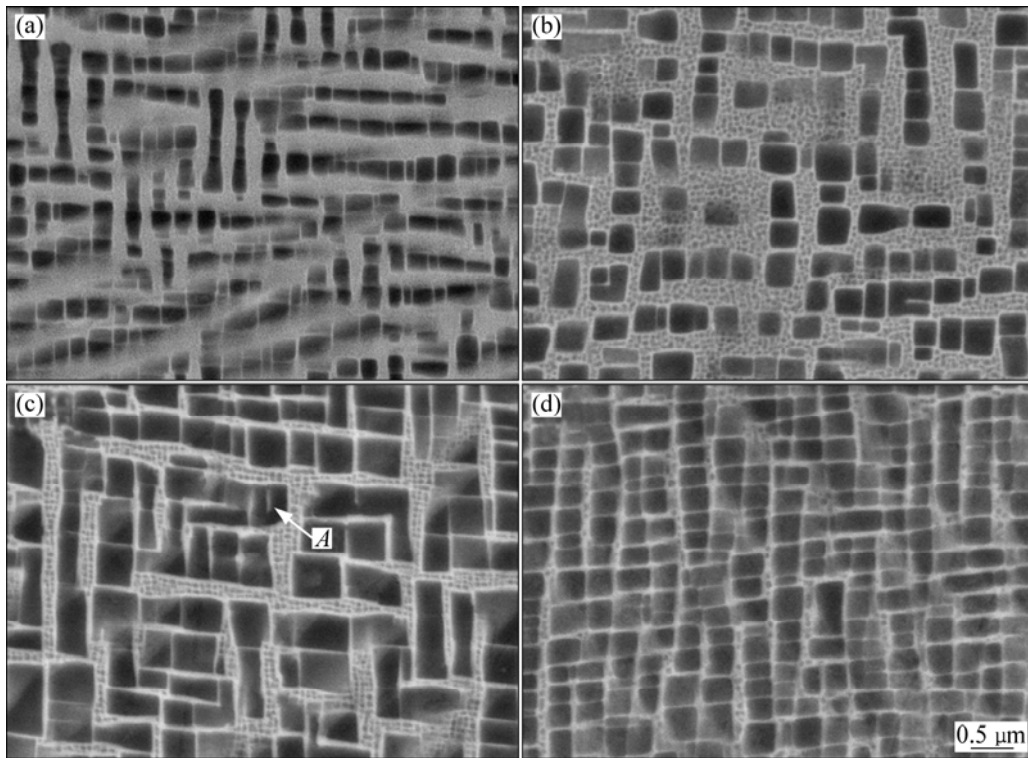


Fig. 2 BSE micrographs of γ/γ' microstructures after the first-step (a) and the second-step aging for 25 h (b), 35 h (c) and 40 h (d) (Bright area is γ matrix and dark area is γ' phase)

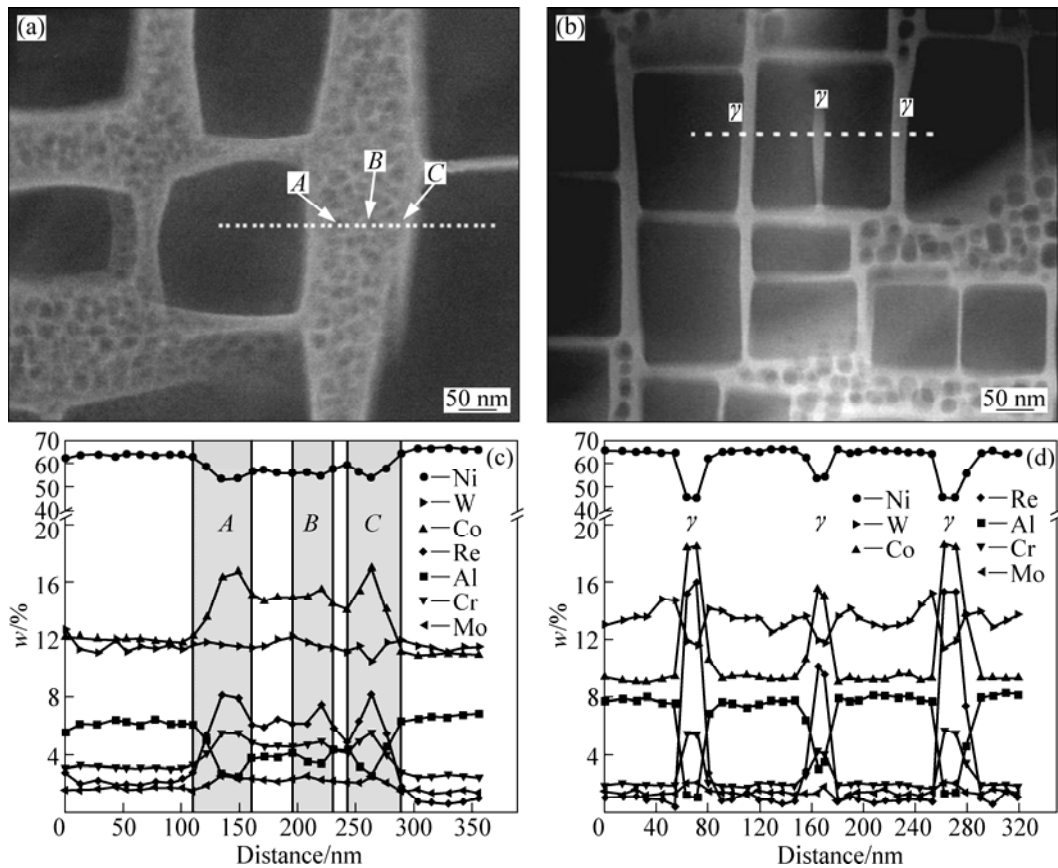


Fig. 3 Dark-field STEM micrographs of γ/γ' microstructures after the first-step aging (a) and the second-step aging for 25 h (b), composition profiles (c), (d) along white lines in (a) and (b), respectively

Fig. 3(c)). This chemical character is similar to that of the γ' phase. It is believed that these fine γ' precipitates were formed during the air cooling at the first-step aging. Figure 3(b) shows a needle-shaped γ precipitate in the cuboidal γ' phase. An EDS analysis across the γ (including the needle-shaped γ phase) / γ' interface clearly indicates that the alloying elements of Re, Co, Cr and Mo are rich in the γ matrix and the needle-shaped γ phase, whereas Al and Ni are rich in the γ' phase (Fig. 3(d)). There is a certain enrichment of W in the vicinity of the γ/γ' interface. Furthermore, the contents of Re, Co, Cr and Mo in the needle-shaped γ phase are obviously lower than those in the γ matrix. Hence, the needle-shaped γ phase probably precipitated within the γ' phase during the second-step aging.

4 Discussion

The γ/γ' microstructures of the alloy after the first-step and the second-step aging show three basic characteristics: 1) the cuboidal γ' phases precipitate during the first-step aging and coarsen modestly during the second-step aging for 25 h; 2) interestingly, the sizes of the cuboidal γ' precipitates first increase and then decrease with the extension of the second-step aging time; 3) the fine spherical γ' phases start to precipitate during the air cooling after the first-step aging and further precipitate/grow to about 50 nm during the second-step aging for 25 h.

According to JMatPro calculation, the misfit of the γ/γ' interface estimated from the equilibrium lattice constants of the two phases, is about -0.41% during the first-step aging. Further precipitation of the γ' phases in the residual γ region in the second-step aging results in a misfit of about -0.05% . According to MÜLLER et al [14], a relatively large misfit between the γ/γ' phases would lead to the γ' precipitation in the cuboidal shape to decrease the total energy as large as possible. Since the coherent strain energy at the γ/γ' interface is almost negligible, the interfacial energy which is proportional to the interface area may be dominant for the morphology formation during the second-step aging. Thus, the γ' phase would precipitate in spherical shape which bears the lowest surface area under a given volume, as shown in Figs. 2(b), (c) and (d).

During the precipitation, there is a repartitioning of the alloying elements in the γ/γ' phases, where a kinetic process is required to reach local equilibrium through short distance diffusion. The equilibrium elemental concentration in the γ/γ' phases at the temperature of the second-step aging (870 °C) calculated with JMatPro is illustrated in Fig. 4. In agreement with the experimental observations, Re, Co and Cr are strongly concentrated in the γ phase, while Mo partitions less strongly to the γ

phase. Ni and Al are enriched in the γ' phase. However, in contrast to JMatPro calculation that W is slightly enriched in the γ phase, the present experimental observation found that W is slightly enriched in the γ' phase (Fig. 3(d)). Moreover, the enrichment of W in the vicinity of the γ/γ' interface was also observed (Fig. 3(d)). It is understood that when γ' precipitate grows in the γ matrix, W is extracted to the γ region. However, since the diffusivity of this element is limited (10^{-17} m²/s at 900 °C [15]), full thermodynamic equilibrium cannot be obtained during the limited period of aging. This explains the discrepancy between thermodynamic calculation and experimental observations.

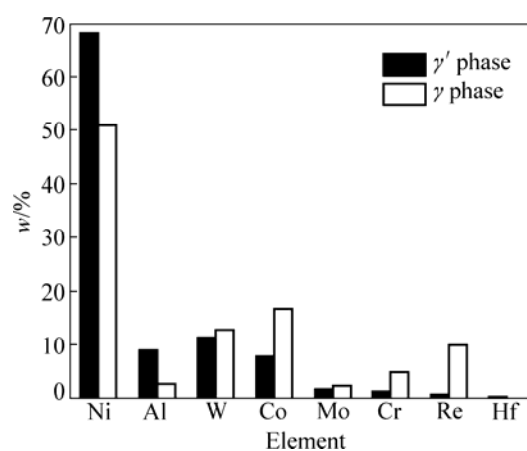


Fig. 4 Elemental distribution between γ and γ' phases at temperature of the second-step aging (870 °C) calculated with JMatPro

Coarsening of the γ' phase during long-term service is a problem for Ni-based superalloy [16]. During the second-step aging, the present observation found that the size of cuboidal γ' phase first increased and then decreased with the increase of aging time. Since the solubility of the alloying elements in the γ/γ' phases changes as a function of temperature, some γ forming elements are supersaturated in the γ' phase while some γ' forming elements are supersaturated in the γ region during the second-step aging. Thus, further precipitation of spherical γ' phases was observed in the γ region. For the similar reason, further precipitation of γ phase within cuboidal γ' phase (phase separation) is also possible. This is evidenced by the needle-shaped γ phase within the γ' phase observed in the microstructure (Fig. 3(c)). Cutting by the needle-shaped γ phase through coarse cuboidal γ' precipitates may help to refine γ' precipitates. Detail of phase separation in Re-containing superalloys are a subject for further investigation.

5 Conclusions

1) The as-grown microstructures of the crystals are

rather uniform. No obvious dendrite is found in the as-grown crystals by the FZ method.

2) Both cuboidal and spherical γ' precipitates are formed after a two-step aging. Precipitation of the spherical γ' phase in the γ matrix and the needle-shaped γ' phase in the coarse cuboidal γ' phase occurs during the second-step aging. Re, Co and Cr are strongly concentrated in the γ phase, while Mo partitions are less strongly to the γ phase. Ni and Al are enriched in the γ' phase.

3) The size of the cuboidal γ' precipitates first increases and then decreases with the extension of the second-step aging time, which could be attributed to phase separation.

References

- [1] HARADA H. High temperature materials for gas turbines: The present and future [C]//Proceedings of the International Gas Turbine Congress. Tokyo: Gas Turbine Society of Japan, 2003: 2–7.
- [2] HU Zhuang-qi, LIU Li-rong, JIN Tao, SUN Xiao-feng. Development of the Ni-base single crystal superalloys [J]. Aeroengine, 2005, 31(3): 1–7. (in Chinese)
- [3] POLLOCK T M, ARGON A S. Directional coarsening in nickel-base single crystals with high volume fractions of coherent precipitates [J]. Acta Metallurgica et Materialia, 1994, 42(6): 1859–1874.
- [4] REED R C. The superalloys: Fundamentals and applications [M]. Cambridge University Press, 2006: 2–20.
- [5] CARON P, KHAN T. Improvement of creep strength in a nickel-base single-crystal superalloy by heat treatment [J]. Materials Science and Engineering, 1983, 61(2): 173–184.
- [6] MURAKUMO T, KOBAYASHI T, KOIZUMI Y, HARADA H. Creep behaviour of Ni-base single-crystal superalloys with various γ' volume fraction [J]. Acta Materialia, 2004, 52(12): 3737–3744.
- [7] NIE J F, LIU Z L, LIU X M, ZHUANG Z. Size effects of γ' precipitate on the creep properties of directionally solidified nickel-base superalloys at middle temperature [J]. Computational Materials Science, 2009, 46(2): 400–406.
- [8] YU Jin-jiang, SUN Xiao-feng, ZHAO Nai-ren, JIN Tao, GUAN Heng-rong, HU Zhuang-qi. Effect of heat treatment on microstructure and stress rupture life of DD32 single crystal Ni-base superalloy [J]. Materials Science and Engineering A, 2007, 460–461: 420–427.
- [9] GIAMEI A, ANTON D. Rhenium additions to a Ni-base superalloy: Effects on microstructure [J]. Metallurgical and Materials Transactions A, 1985, 16(11): 1997–2005.
- [10] KAUNARATNE M S A, CARTER P, and REED R C. Interdiffusion in the face-centred cubic phase of the Ni-Re, Ni-Ta and Ni-W systems between 900 and 1300 °C [J]. Materials Science and Engineering A, 2000, 281(1–2): 229–233.
- [11] HOBBS R A, ZHANG L, RAE C M F, TIN S. The effect of ruthenium on the intermediate to high temperature creep response of high refractory content single crystal nickel-base superalloys [J]. Materials Science and Engineering A, 2008, 489(1–2): 65–76.
- [12] CARROLL L J, FENG Q, MANSFIELD J F, POLLOCK T M. Elemental partitioning in Ru-containing nickel-base single crystal superalloys [J]. Materials Science and Engineering A, 2007, 457(1–2): 292–299.
- [13] FUCHS G E. Solution heat treatment response of a third generation single crystal Ni-base superalloy [J]. Materials Science and Engineering A, 2001, 300(1–2): 52–60.
- [14] MÜLLER L, GLATZEL U, FELER-KNIEPMEIER M. Modelling thermal misfit stresses in nickel-base superalloys containing high volume fraction of γ' phase [J]. Acta Metallurgica et Materialia, 1992, 40(6): 1321–1327.
- [15] REED R C, TAO T, WARNKEN N. Alloys-by-design: Application to nickel-based single crystal superalloys [J]. Acta Materialia, 2009, 57(19): 5898–5913.
- [16] COAKLEY J, BASOALTO H, DYE D. Coarsening of a multimodal nickel-base superalloy [J]. Acta Materialia, 2010, 58(11): 4019–4028.

含铼镍基单晶高温合金阶段时效过程中 γ/γ' 相的 微观组织形貌与化学成分

王 静, 张澜庭, 陈 科, 孙乃荣, 单爱党

上海交通大学 材料科学与工程学院, 上海 200240

摘 要: 利用扫描电子显微镜(SEM)、透射电子显微镜(TEM)和扫描透射电子显微镜(STEM)研究了含铼镍基单晶高温合金经二次时效处理后的 γ/γ' 相微观组织结构。实验所用单晶用悬浮区熔法(FZ)制备。结果表明: 二次时效后合金中有方形和球形 γ' 相析出, 方形 γ' 相的尺寸随着二次时效时间的延长先增大后减小; 合金元素 Re、Co 和 Cr 严重偏聚于 γ 相中, 而 Ni 和 Al 则偏聚于 γ' 相中。并借助 JMatPro 热力学计算软件分析了实验现象。

关键词: 镍基单晶高温合金; γ/γ' 相的微观组织结构; 元素分布; 热处理; JMatPro 计算

(Edited by YANG Hua)